Smart Structures and Systems, *Vol. 27, No. 3 (2021) 467-478*
DOI: https://doi.org/10.12989/sss.2021.27.3.467

Seismic behavior of a two-level control system with double vertical shear links in series

Mohsen Zare Golmoghany [1] and Seyed Mehdi Zahrai*[1,2]

[1] *School of Civil Engineering, College of Engineering, University of Tehran, Tehran, Iran*
[2] *Department of Civil Engineering, University of Ottawa, Canada*

(*Received June 25, 2020, Revised October 5, 2020, Accepted November 29, 2020*)

Abstract. To improve seismic behavior of structures, a two-level control system is proposed in this paper where by combining two vertical shear panels in series in a chevron bracing configuration, Double-Vertical Shear Panel, D-VSP is introduced. Utilizing two-levels of energy absorption for two different earthquake intensity levels, D-VSP is expected to beneficially change dynamic behavior parameters like strength, stiffness and damping ratio through increasing ductility. To validate research, a VSP is modeled in ABAQUS and related numerical results are compared to those of a previous experimental work. Pushover, quasi-static cyclic and seismic analyses are conducted on two models. The hysteresis curves show symmetric two-level behavior with stable strength and stiffness leading to increase ductility ratio up to 29.4%. Maximum displacement and maximum base shear under seismic loading decrease 5.91 and 11.18% respectively under moderate earthquakes when D-VSP system uses only first fuse, saving second fuse for severe earthquakes. However, in a strong earthquake, both of the shear panels absorb seismic energy and can control vibration better than conventional systems with one level control mechanism. The proposed system using a weaker panel can better control an extensive range of earthquakes as well as the earthquake with foreshocks.

Keywords: Chevron bracing; cyclic behavior; energy dissipation; vertical shear link; two-level control system; seismic response

1. Introduction

Seismic control systems have been used since the 1980s (Soong and Dargush 1997). Several researchers studied energy absorption systems to control seismic vibration in the last decades (Silwal *et al*. 2015). Dampers according to functional nature are categorized into three types of passive (Zahrai and Jalali 2014), semi-active (Symans and Constantinou 1999, Ying *et al*. 2009), and active control (Preumont 1999, Casciati *et al*. 2012, Mait *et al*. 2006), from which passive dampers are more typically implemented because they are easy to be fabricated and do not need external energy for dissipating earthquake energy (Ghamari *et al*. 2019). Yielding damper is a kind of passive control that absorbs seismic energy through inelastic deformations. The shear link beam is a kind of yielding damper that first was used to create an opening for architectural purposes (Roeder and Popov 1978), but its benefits were later confirmed for energy dissipation (Lian *et al*. 2015). The Vertical Shear Panel (VSP) implemented between chevron braces and the flange of floor beam was proposed by Seki *et al*. (1988) in a two-story frame, leading to appropriate cyclic behavior with stable and reliable hysteresis curves. Zahrai and Bruneau (1999) studied VSP in slab-on-girder bridges and showed that this damper could increase ductility and energy dissipation in such bridges. The length of the link in VSP is a most important aspect in its ductile behavior and nonlinear response (Duan and Su 2017). When link length is short, shear yielding will dominate in the inelastic response while for long link, moment yielding dominates in structural response (AISC 2005, Zahrai and Moslehi Tabar 2006). To improve seismic behavior of VSPs, researchers used different materials for VSP (Rai *et al*. 2013, Lian and Su 2018). Li *et al*. (2020) and Lian and Su (2017a) studied on frames with VSP which were made of high-strength steel showing a similar bearing capacity to ordinary steel while reducing the construction cost. To maintain a shear or moment yielding and to improve seismic behavior of vertical panels, researchers used panel with different shapes. For example, Lee *et al*. (2015) introduced a non-uniform steel strip damper and showed stress concentration reduction in panel leading to a ductile failure in structure. Efficacy of VSP length and thickness was studied by Zahrai and Moslehi Tabar (2006) who found that link section depth, web thickness and panel length have a direct impact on dynamic characteristics such that increasing web thickness, web depth and using short panel improved seismic energy dissipation. To predict the VSP hysteretic response, some researchers suggested mathematical models (Zahrai and Moslehi Tabar 2013, Hossain and Ashraf 2012, Hossain *et al*. 2011). Shear panel with web stiffener was also studied by Nakashima *et al*. (1994) showing stable hysteresis curves and more energy dissipation increasing by 50% using stiffeners. Zahrai (2015) assessed the influence of stiffener on VSP. He tested

*Corresponding author, Professor,
E-mail: mzahrai@ut.ac.ir

ISSN: 1738-1584 (Print), 1738-1991 (Online)

5 specimens with different beam, column, brace, and VSP sections and used stiffeners in some specimens and achieved that using stiffener increases structural ductility and damping ratio up to 26.7-30.6%. The vertical panels have been useful in both steel and concrete structures. To control residual drift and to improve the lateral load-resisting capacity in concrete frames, Oinam and Sahoo (2018a, b) used VSPs. Lian and Su (2017b, c) conducted a shake table test on three-story frame equipped with VSP and showed that VSP act as a fuse experiencing damages while other members remain elastic, in general leading to reliable hysteretic behavior and seismic performance. Lian *et al*. (2017) showed that SAP2000 provided a very accurate prediction of the structure with VSP under seismic loading.

In recent years, many researchers have proposed new systems in which different dampers are combined to improve seismic behavior in terms of deformation, ductility and energy dissipation capacity (Buravalla and Bhattacharya 2007, Makihara 2012, Sahoo *et al*. 2015, and Wei *et al*. 2019). Zahrai and Vosooq (2013) suggested chevron knee bracing and shear panel in series connection. They showed that the proposed system has two fuses in hysteresis curve leading to increase ductility capacity in the structure. Cheragi and Zahrai (2017) suggested a two-level pipe damper used in a diagonal brace. In a moderate seismic event, outer pipe starts to absorb energy while in strong earthquakes, deformations in the outer pipe stop and inner pipe begins to dissipate energy. Their systems had suitable energy dissipation, ductility and stable hysteresis. A combination of two fiction damper and non-uniform strip damper was proposed by Lee *et al*. (2016) finding that this system had stable hysteresis response with more plastic deformation and energy dissipation capacity. In another study, Hosseini Hashemi and Moaddab (2017) investigated nonlinear behavior of the hybrid system of steel-plate yielding and friction damper with high ductility enabling the system to properly absorb energy in moderate and strong earthquakes. Rousta and Zahrai (2017) investigated experimental and numerical behavior of a new system as a combination of a chevron knee brace and a VSP acting in a two-level control system. Their research showed earlier absorbing energy with increasing strength and energy dissipation capacity. Cheragi and Zahrai (2017) studied a two-level pipe damper used in 5, 10 and 15-story steel buildings and showed reduction of roof displacement and acceleration compared to the frame without damper. Ranaei and Aghakouchak (2018) investigated hybrid damper consisting of viscoelastic and flexural yielding strip dampers and found that the system is useful for strong and moderate earthquakes while viscoelastic and flexural yielding strip dampers compensate some shortcomings.

In this paper, a Double –Vertical Shear Panel (D-VSP) is proposed as a kind of two-level control system. It is located between the apex of chevron bracing and flange of the floor beam. This system consists of two VSPs in series benefiting from two control fuses corresponding to two levels of seismic events. Upper part (U-VSP) is weaker than lower part (B-VSP) hence plastic deformation in U-VSP begins earlier. Stopper bolts can change energy absorbing panels at a specific displacement. So this system can dissipate seismic energy in two levels without decreasing strength and stiffness while delaying the yield in the 2nd fuse (stronger shear panel) and can control and decrease base shear, maximum displacement and permanent lateral displacement under different earthquakes. To investigate cyclic and seismic behavior, firstly, previous experimental results are used to validate the finite element analysis developed by ABAQUS software. Then to obtain performance of D-VSP, pushover analysis is conducted on three models and finally cyclic behavior and seismic response under earthquake excitation are obtained.

2. Proposed system definition

2.1 Double –VSP

The D-VSP consists of two vertical link beams in series such that one link beam is above the other. The lower shear panel is stronger such that the upper member is yielding earlier than the lower part. Vertical panels are connected together using a UNP segment on which there are 4 openings and bolts. Bolts can have certain limited displacement inside holes to control displacement of U-VSP. When the bolts are at one end stuck by UNP section, sliding plates sustain the lateral load preventing the top shear panel to experience further deformations so B-VSP as the 2nd fuse can enter plastic deformation range and related energy absorption (Fig. 1). Therefore, this system can dissipate energy in two levels. The other benefit of this

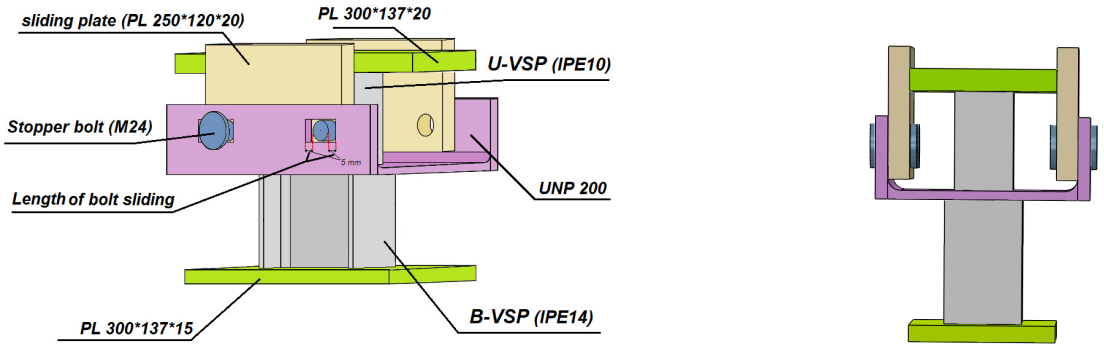

(a) (b)

Fig. 1 Details of D-VSP damper

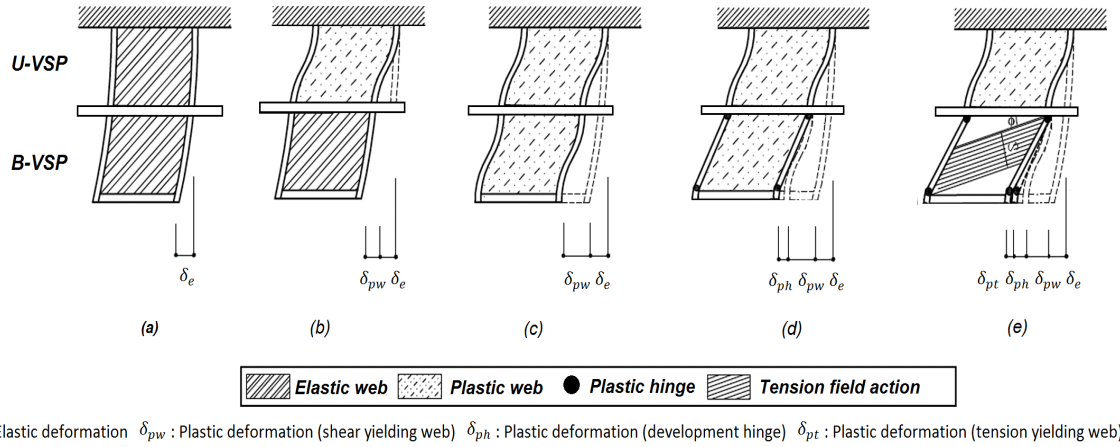

Fig. 2 Lateral performance of D-VSP under increasing lateral load

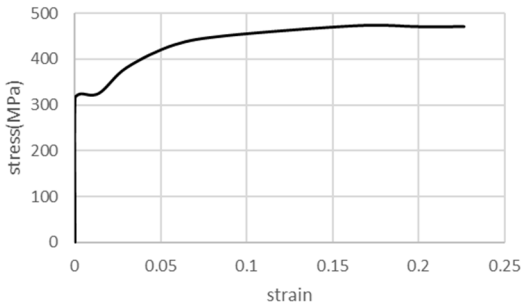

Fig. 3 Tensile stress–strain response of steel

system is that the D-VSP has simple structure and can be easily implemented above the chevron bracing.

Performance of D-VSP damper with increasing lateral load is shown in Fig. 2. Firstly, displacement of panels is in elastic range then in second and third stages web of U-VSP and B-VSP panels yield respectively. In the fourth stage, flexural plastic hinges are created in bottom panel and at the end, the web at B-VSP reaches maximum plastic deformation and shear buckling such that it loses stiffness when one can assume lateral load is resisted by tension field action (Zahrai and Tabar 2013).

2.2 Material property

All steel members used in this research have yielding stress of 320 MPa and ultimate stress of 482.2 MPa with Stress-Strain curve as shown in Fig. 3. The Young's modulus and the Poisson's ratio are 21000 MPa and 0.3 respectively. All members are assumed to show isotropic behavior where kinematic hardening model was adopted to simulate the shear panels in all cases.

2.3 Lateral loading

The quasi-static load that is used in this paper was developed based on the ATC-24 (Krawinkler 1992). In this Guideline, three times displacement cycles at 0.125, 0.25, 0.5, 1, 2, and 3 times of yield displacement (Δ_y) and then 2 cycles until maximum displacement are applied to the system. The cyclic loading is shown in Fig. 4.

3. Design basis and validation

3.1 Design of stopper bolts and connection plates

The VSP must have shear inelastic deformation according to AISC 341 (2010) and the length of shear panel shall be

$$e \le 1.6\frac{M_P}{V_P}. \quad M_P = ZF_y. \quad V_P = 0.6\,F_y d t_w \tag{1}$$

Where e, Z, d, and t_w are the length, plastic modulus, section depth and the web thickness of VSP, respectively. The proposed VSP model consists of two panels in series and to have shear yielding dominance in inelastic response, Eq. (1) is expanded as follows

$$e_b \le 1.6\frac{M_{Pb}}{V_{Pb}}, M_{Pb} = Z_b F_y, V_{Pb} = 0.6\,F_y d_b t_{w_b} \tag{2}$$

$$e_t + e_b \le 1.6\frac{M_{Pt}}{V_{Pt}},\ M_{Pt} = Z_t F_y, V_{Pt} = 0.6\,F_y d_t t_{w_t} \tag{3}$$

In the above equations t and b subscripts show details for top and bottom panels respectively. Based on the above

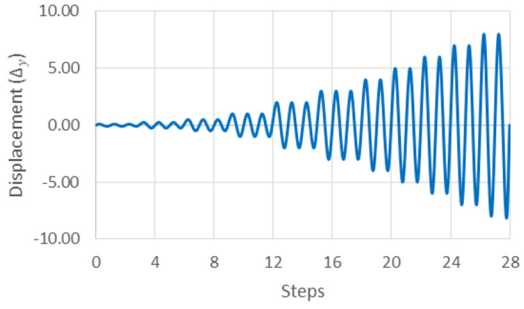

Fig. 4 Applied lateral displacement protocol according to ATC-24 (1992)

equations, IPE140 and IPE100 are chosen for lower and upper panels, respectively. Therefore, the total length of panels is 20 cm from which the length of U-VSP and B-VSP are 5 cm and 15 cm, respectively.

3.2 Stopper design

Stopper bolts, sliding plates, and UNP segment are important parts to absorb energy in two-level scenario so it is necessary that they be designed to prevent U-VSP from large plastic deformation and thus to activate B-VSP as the 2nd damper. The sliding plates are welded to the top plate and are connected by bolts to the UNP segment. The connection surface between sliding plates, bolts, and the UNP segment are assumed frictionless with hard contact (Fig. 1). Also, the pre-loads in bolts are assumed zero which act only as stoppers without interfering in the performance of the D-VSP first fuse.

Maximum load applied to the bolts and sliding plates is the difference between load-carrying capacities of two panels. Therefore, four bolts of class 8.8 with a diameter of 24 mm are used. Sliding plates and the UNP section are designed according to block shear as presented in Fig. 5.

The sliding length for the bolts (Fig. 1) is chosen based on maximum plastic deformation for U-VSP that can be used for the total energy dissipation capacity of the U-VSP without any rupture in the B-VSP. Maximum plastic deformation (Δ_u) in U-VSP based on Zahrai and Tabar (2013) is

$$\Delta_u = \frac{\sqrt{3}}{2}\left(1+\frac{1}{12}\left(\frac{1-2\upsilon}{1-\upsilon}\right)^2\left(\frac{{d_t}^2 t_{wt} e_t}{I_t}\right)^2\right)^{-0.5}\varepsilon_u e_t \quad (4)$$

Where υ is the Poisson's ratio, I_t is the moment of inertia of the U-VSP section and ε_u is the steel ultimate strain under uniaxial tension.

The sliding length must be smaller than maximum plastic deformation so the sliding length is chosen 3.4cm that due to the bolt diameter, U-VSP experiences relative deformation of 1 cm.

3.3 Design of frame main members

All others members such as columns and beam must remain in elastic range during lateral cyclic loading. Brace is designed for maximum pressure without buckling so section area for braces (A_{br}) is

$$A_{br} \geq \frac{F_u d_b t_{w_b}}{2F_{cr} * \sin(\theta)} \quad (5)$$

Where F_u, F_{cr} and θ are ultimate stress, brace critical buckling stress and angle between brace and column, respectively.

Therefore, IPB120, IPB140, and 2UNP80 sections are chosen for columns, beam and braces. Gap between 2UNP80 is 1 cm while batten plates of 10*3*1 cm are used in between at spacing of 54 cm.

3.4 Numerical model validation

In this paper, to validate numerical models, a previous experimental work on I-shaped VSP with web stiffener in chevron braced frame studied by Zahrai (2015) is used. The finite element analysis by ABAQUS 6.14 (2014) software is used to get numerical results for SPS2 specimen as shown in Figs. 6(a) and (b). The lateral loading is applied to the frame according to ATC-24 that is shown in Fig. 4. Section details and the length for frame members are given in

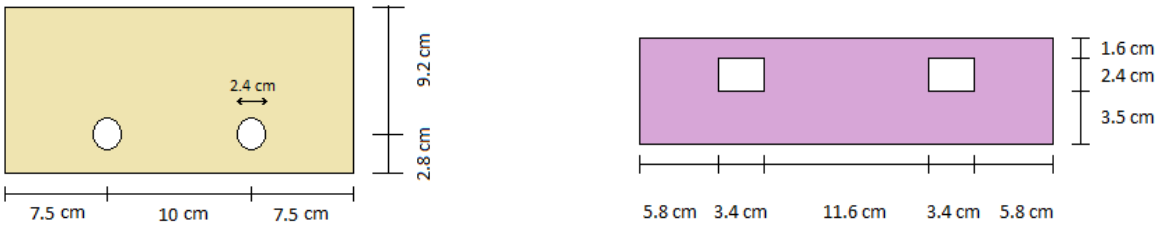

(a) Sliding plate (b) UNP200 flange

Fig. 5 Details of the sliding plates and UNP200 flange

(a) (b)

Fig. 6 (a) Experimental specimen (Zahrai 2015); and (b) numerical model

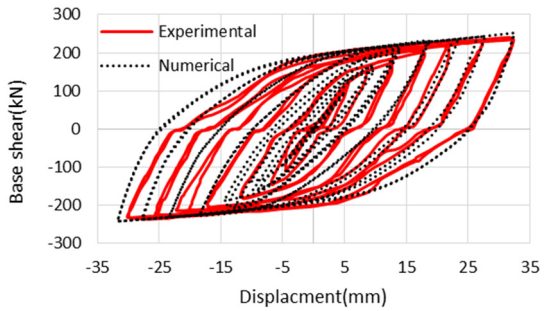

Fig. 7 Hysteresis curves of Experimental and numerical model for SPS2

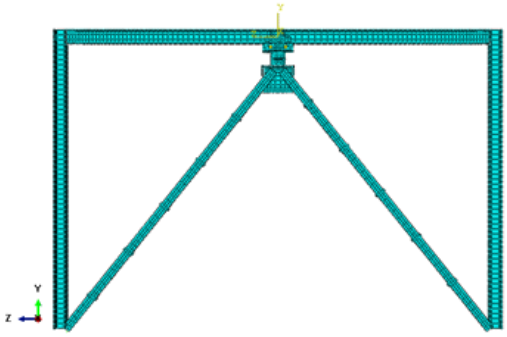

Fig. 8 D-VSP model in Abaqus

Table 1. The experimental and numerical results are shown in Fig. 7 where a comparison between their hysteresis curves confirms the correctness of modeling the main frame, dimension and member properties, connections, lateral load, boundary conditions and model meshing. The little difference between experimental and numerical results can be due to ignoring details of welded and bolted connections.

4. Numerical modeling and analysis

The effect of the proposed damper on the structural ductility is studied by ductility ratio, μ, whose value is defined by

$$\mu = \frac{\Delta_{max}}{\Delta_y} \tag{6}$$

Where, Δ_{max} and Δ_y respectively are maximum lateral displacement, and yield displacement. So, ductility ratio for the S1 model is 10 and for the S2 case is 7.73, which means it increases by 29.4% in the new proposed system.

4.2 Quasi-static cyclic loading result

The hysteresis behavior under cyclic loading according to ATC-24 protocol (Fig. 4) for D-VSP is shown in Fig. 11 showing symmetrical hysteresis behavior without strength and stiffness degradation. According to Fig. 11(a), the weaker shear panel (U-VSP) first experiences the plastic behavior, which is responsible for seismic energy dissipation in moderate earthquakes, while the stronger panel (B-VSP) remains intact to resist severe earthquakes. In a stronger earthquake, stopper bolts are locked by UNP and the shear force is transferred by bolts to the bottom panel (B-VSP) while bolts prevent increase of displacement in the U-VSP, which results in shear force increase in B-VSP and onset of energy dissipation in this panel, which is observed as a force jump in hysteresis curve of S1 (Fig. 11(a)).

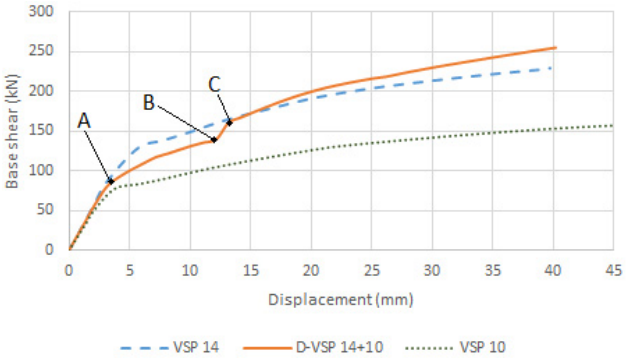

Fig. 9 Pushover curves for S1(orange), S2(blue) and S3(green)

Table 1 Details of test specimen for validation purposes

	Column	Beam	Brace	Vertical shear panel	Panel and web Stiffeners
Section	IPB120	IPE140	2UNP80	IPE140	Plate with 10 mm thickness
Length	300 cm	420 cm	345 cm	20 cm	

Table 2 Properties of three models considered in this study

Sample		**Column**	**Beam**	**Brace**	**U-VSP**	**B-VSP**
S1 (D-VSP14+10)	Section	IPB120	IPE140	2UNP80	IPE10	IPE140
	Member length	300 cm	420 cm	345 cm	5 cm	15 cm
S2 (VSP14)	Section	IPB120	IPE140	2UNP80	-	IPE140
	Member length	300 cm	420 cm	345 cm	-	20 cm
S3 (VSP10)	Section	IPB120	IPE140	2UNP80	-	IPE10
	Member length	300 cm	420 cm	345 cm	-	20 cm

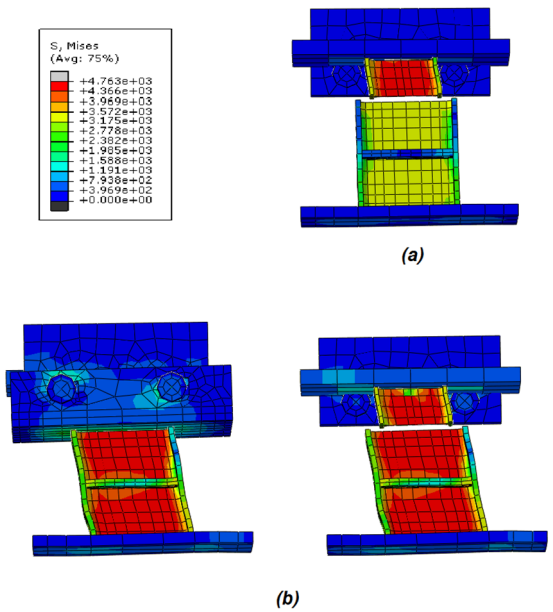

Fig. 10 Details of VLB stress distribution (a) First fuse; (b) Second fuse with and without UNP segment

According to the curves (Fig. 11), this system can dissipate earthquake energy in two levels which is stable in all cycles. The maximum load-carrying capacity for the S1 model is 267 kN while those values for the S2 and S3 models are 233 kN and 162 kN showing an increase by 14.6% and 64.8%, respectively. The energy dissipations of those three models are shown in Fig. 12. The energy graph shows improved behavior for S1 compared to S3 increasing 36.6% but a 9.5% decrement of energy dissipation at S1 compared to S2 which was predictable because S1 has a weaker member. The equivalent viscous damping ratio regarding the hysteresis curve is calculated according to Eq. (7).

$$\xi_{eq} = \frac{A_h}{2\pi V_m \Delta_m} \tag{7}$$

Where A_h, V_m and Δ_m are area of under each hysteresis cycles, the average of maximum forces and the average of maximum displacement in a complete cycle of the cyclic curve, respectively. All hysteresis cycle damping ratios are calculated and shown in Fig. 12. The proposed D-VSP in low displacement has higher damping ratio than the S2 and similar to the S3 but after activating the second fuse, damping ratio in S1 is decreased due to stair-step hysteresis curves in which the average of maximum forces increases creating slightly less damping ratio.

4.3 Seismic analysis

4.3.1 Far-field earthquakes

In this section, seismic performance of the S1, S2 and S3 models are presented. For this purpose, the accelerations of the Bam, Imperial Valley, and Tabas earthquakes are chosen such that their PGAs (Peak Ground Accelerations)

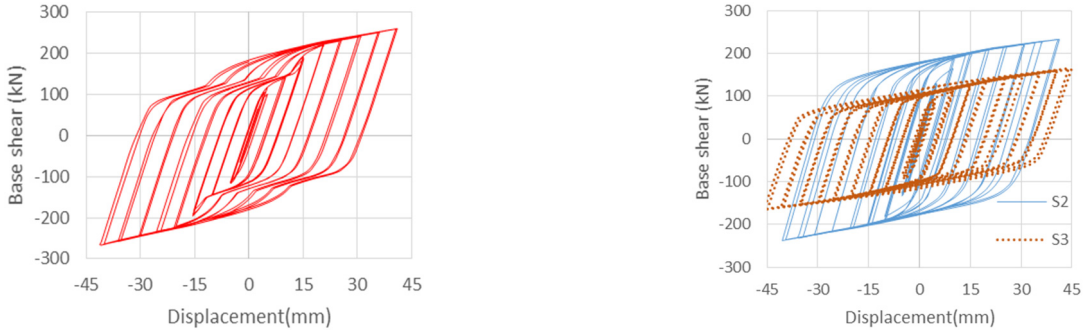

Fig. 11 Hysteresis curve of the chevron braced frames with shear panel models: (a) S1; (b) S2, S3

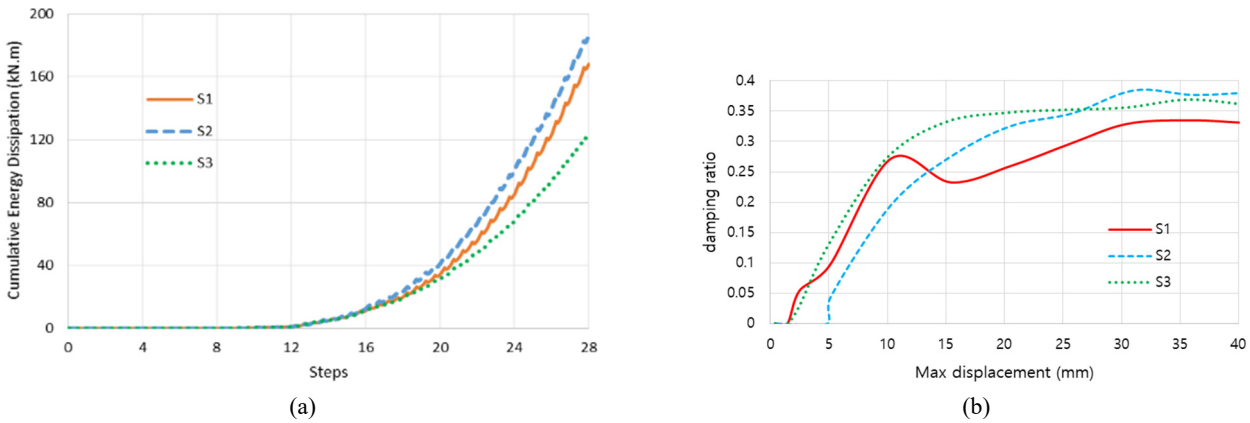

Fig. 12 (a) Cumulative dissipated energy; (b) Damping ratios of models

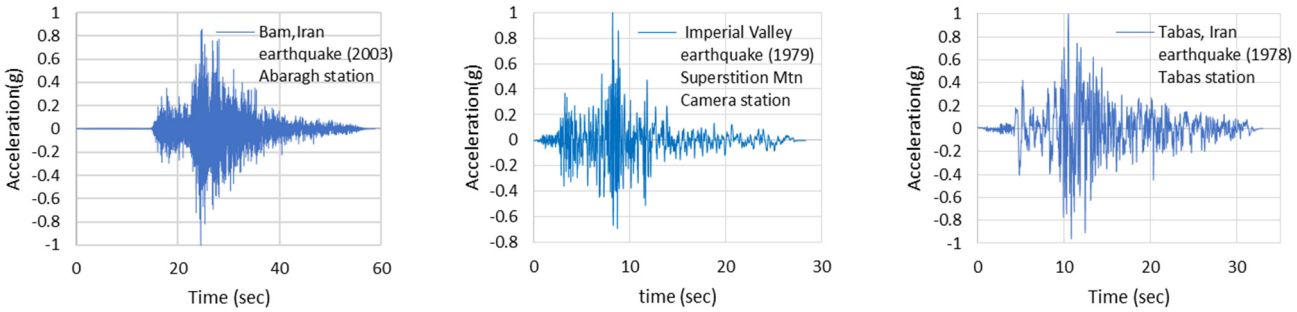

(a) (b) (c)

Fig. 13 Far-field earthquakes scaled to gravity acceleration: (a) Bam (b) Imperial Valley (c) Tabas

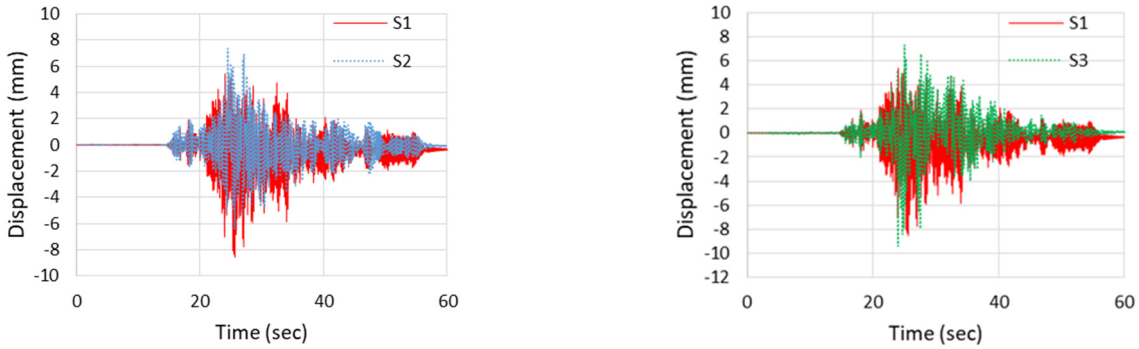

(a) (b)

Fig. 14 Displacement responses under the Bam earthquake: (a) S1-S2; (b) S1-S3

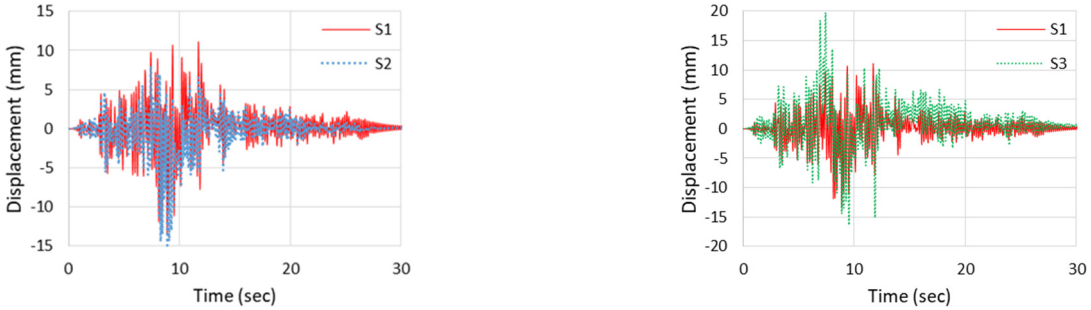

(a) (b)

Fig. 15 Displacement responses under the Imperial Valley earthquake: (a) S1-S2; (b) S1-S3

(a) (b)

Fig. 16 Displacement responses under the Tabas earthquake: (a) S1-S2; (b) S1-S3

Table 3 Seismic response for the S1 and S2 models under far-field earthquakes

Earthquake	Model	Maximum displacement (mm)	Maximum base shear (kN)
Bam	S1	8.56	126.25
	S2	7.36	157.08
	S3	9.41	98.02
Imperial Valley	S1	13.46	153.27
	S2	14.93	190.01
	S3	19.79	119.06
Tabas	S1	21.81	222.57
	S2	28.77	211.14
	S3	44.75	151.63

are scaled to 1 g. Scaled acceleration records are shown in Fig. 13. For dynamic analysis, a 20ton-mass is assumed at the beam to which earthquake accelerations are applied. Responses of seismic analysis are summarized in Table 3 and displacement results are shown in Figs. 14-16. For example, according to the Imperial Valley seismic response, maximum displacement in the S2 model is 14.93 mm while using the proposed D-VSP, the maximum displacement decreased 9.85% reaching 13.46 mm such that maximum base shear decreased 19.33%.

According to Table 3, the proposed two-level damper can control the seismic vibrations such that all other members like columns, beam and braces remain elastic. Compared to S2 and on average, maximum displacement and maximum base shear using the proposed system decreased 5.91%, and 11.18%, respectively. According to Table 3, under moderate earthquakes like the Bam earthquake using a weaker panel and thus a lower force, the S1 model can control seismic behavior so it leads to decreasing structural damages under moderate events. Also using the participation of the B-VSP, the proposed system can control seismic vibrations better than S3 under strong earthquakes. On average, maximum displacement decreased 30.8% in the S1 model compared to that in the S3 model.

According to hysteresis curves under the Bam earthquake (Fig. 17(a)), at S1 model only U-VSP yields and B-VSP (main panel) remains elastic reducing base shear in structure. As observed in Fig. 17(b) for hysteresis curve under the Imperial Valley earthquake, bolts are to engage with the plates inducing a bit more shear force but there is still no yield in the B-VSP. On the other hand, under the Tabas earthquake (Fig. 17(c)) both panels absorb seismic energy while under those three earthquakes in the S2, the main panel is in charge of energy dissipation. Therefore, although the weaker panel is used in D-VSP, performance under moderate earthquakes is somewhat better than the case with only one VSP, at the same time saving the second fuse for the strong shock.

According to hysteresis curves for the S1 under the far-field earthquakes (Fig. 17), the proposed system has symmetric behavior in terms of displacement because S1

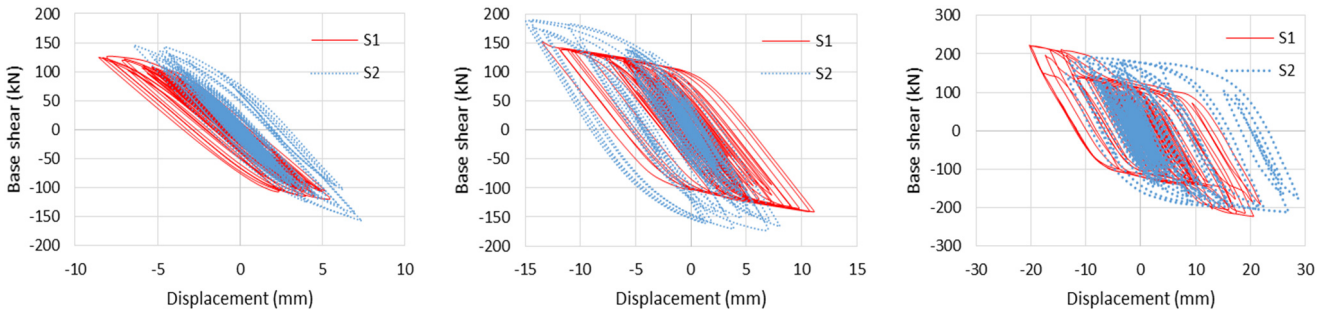

(a) (b) (c)

Fig. 17 Hysteresis curves for earthquake responses: (a) Bam; (b) Imperial Valley; (c) Tabas

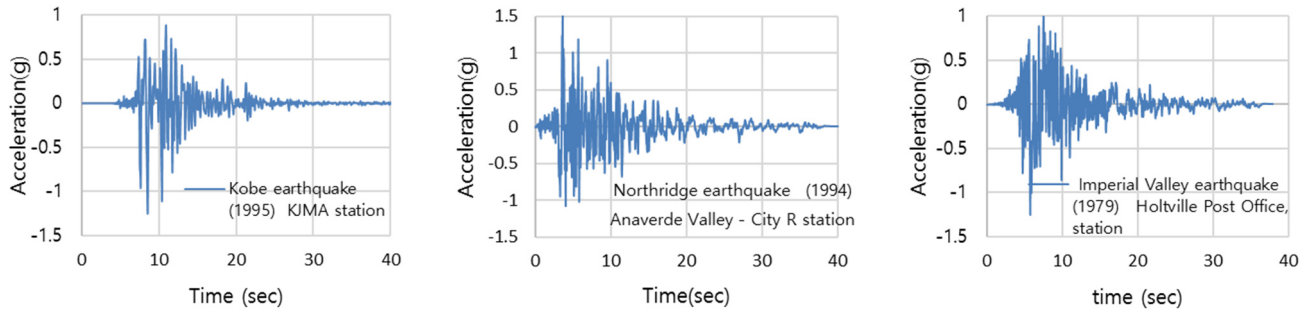

(a) (b) (c)

Fig. 18 Near-field earthquake acceleration records: (a) Kobe; (b) Northridge; (c) Imperial Valley

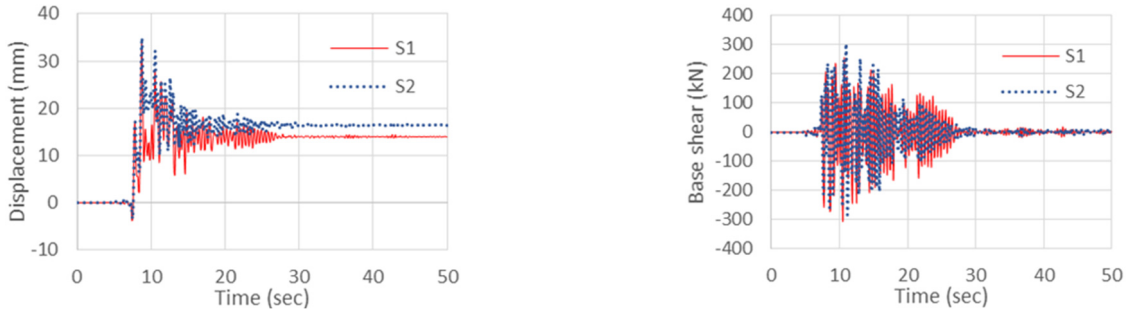

(a) (b)

Fig. 19 Responses of the S1 and S2 models under the Kobe near-field earthquake: (a) displacement; (b) base shear

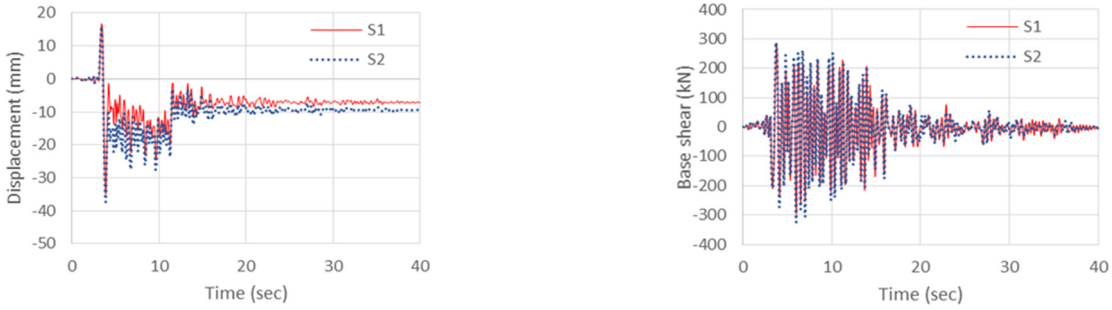

(a) (b)

Fig. 20 Responses of the S1 and S2 models under the Northridge near-field earthquake: (a) displacement; (b) base shear

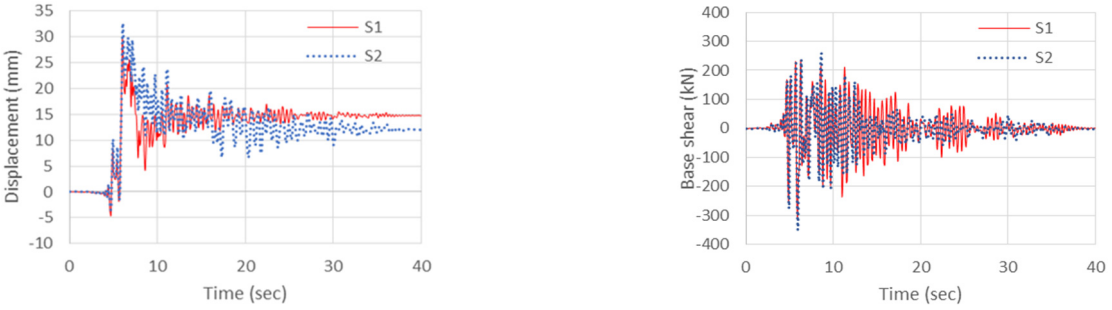

(a) (b)

Fig. 21 Responses of the S1 and S2 models under the Imperial Valley near-field earthquake: (a) displacement; (b) base shear

yields sooner than S2 and uses all weaker panel potential capacity, and then the main panel absorbs seismic energy if needed. Due to symmetric displacements at cyclic loading for the S1 and less participation of stronger panel in energy dissipation, maximum base shear decreases under moderate earthquakes.

4.3.2 Near-field earthquakes

To study seismic performance of the proposed system under stronger earthquakes, near-field records of the Kobe, Northridge, and Imperial Valley earthquakes which are scaled up as shown in Fig. 18 are used. According to PGA for near-field earthquakes, these earthquakes are stronger than far-field earthquakes. Responses from seismic analysis are summarized in Table 4 and are shown in Figs. 19-21. All near-field earthquake results for S3 show that VSP ruptures and cannot resist lateral loading. According to the results, on average, maximum displacement, permanent displacement and maximum base shear using the proposed system

Table 4 Seismic response for the S1 and S2 models under near-field earthquakes

Earthquake	Case	Maximum displacement (mm)	Permanent displacement (mm)	Maximum base shear (kN)
Kobe	S1	33.74	13.93	302.93
	S2	34.98	16.54	301.39
Northridge	S1	34.81	7.12	294.28
	S2	37.24	9.59	322.07
Imperial Valley	S1	29.28	14.73	314.08
	S2	32.23	11.94	350.06

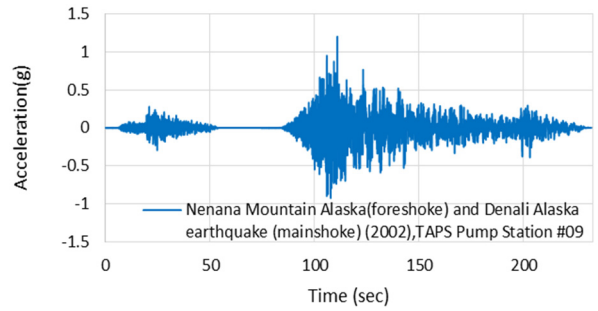

Fig. 22 The Alaska earthquake foreshock and main shock record

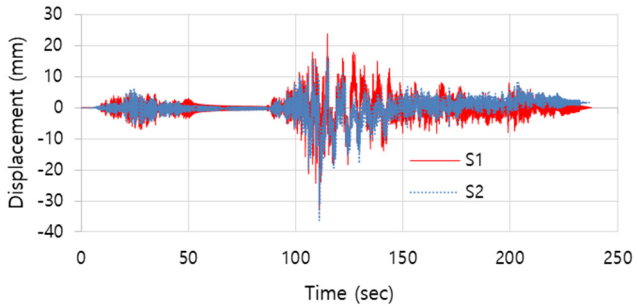

Fig. 23 Displacement response of the S1 and S2 under the Alaska foreshock and main shock

decreased 6.41%, 6.06% and 6.13%, respectively. The two-level damper can control the structures against strong earthquakes somewhat better than just yielding one VSP alone. So, the proposed system not only causes disorder the performance of the structure in stronger earthquakes it also can decrease structural response.

4.3.3 Earthquakes with foreshock

To study performance of the proposed system under an alternate earthquake with foreshock and aftershock, the Alaska earthquake is applied to S1 and S2. Scaled up record for this earthquake is shown in Fig. 22. Displacement history for S1 and S2 models under the Alaska earthquake is shown in Fig. 23. Maximum displacement at foreshock for S1 is 7.04 mm so only U-VSP yields while B-VSP remains elastic. On the contrary, maximum displacement at S2 is 6.47 mm and the VSP experiences plastic behavior. Under main records, maximum displacement decreases 8.8% and permanent displacement decreases from 1.75 mm to 0.015 mm. So, the proposed system by saving B-VSP in foreshock has better performance in the main earthquake.

5. Conclusions

In this paper, a two-level control system called D-VSP, consisting of two VSPs in series, was proposed and its seismic performance was investigated. With simple structure, this system can be easily implemented above the chevron bracing system. The hysteresis curve represents a symmetric two-level behavior with variable strength and stiffness that can dissipate energy in different earthquake levels. Numerical response to cyclic and seismic loading under two sets of three earthquakes were obtained. Results of this research are summarized as following:

- Ductility ratio for the S1 and S2 models respectively, were obtained 10 and 7.73 showing more ductility in the proposed two-level control system where energy dissipation in D-VSP starts sooner than S2 without decreasing strength and stiffness.
- In the far-field earthquake, the hysteresis curve for D-VSP was symmetrical so by using all energy absorbing capacity at D-VSP compared to S2, maximum displacement and base shear was decreased controlling all earthquakes better than S3 so that on average, maximum displacement decreased 30.8%. The proposed system experienced less yielding in stronger panel under near-field earthquakes, compared to S2 and in average reducing maximum displacement, permanent displacement and base shear 6.4%, 6.1% and 6.1%, respectively while S3 ruptured under near-field earthquakes.
- Under moderate earthquake and foreshock, only weaker panel absorbed energy while stronger panel remained elastic better prepared against probable aftershocks.

References

ABAQUS (2014), Finite Element Analysis Program, Version 6.14.2. User's Manual.

AISC (2005), Steel Construction Manual, American Institute of Steel Construction, 13th Edition, Chicago, IL, USA.

AISC 341 (2010), Seismic Provisions for Structural Steel Buildings, American Institute of Steel Construction, Chicago, IL, USA, June 22.

Buravalla, V.R. and Bhattacharya, B. (2007), "A new hybrid vibration control methodology using a combination of magnetostrictive and hard damping alloys", *Smart Struct. Syst., Int. J.*, **3**(4), 405-422. https://doi.org/10.12989/sss.2007.3.4.405

Casciati, F., Rodellar, J. and Yildirim, U. (2012), "Active and semi-active control of structures–theory and applications: A review of recent advances", *J. Intell. Mater. Syst. Struct.*, **23**(11), 1181-1195. https://doi.org/10.1177/1045389X12445029

Cheraghi, A. and Zahrai, S.M. (2017), "Cyclic testing of multilevel pipe in pipe damper", *J. Earthq. Eng.*, **23**(10), 1695-1718. https://doi.org/10.1080/13632469.2017.1387191

Duan, L. and Su, M. (2017), "Seismic testing of high-strength steel eccentrically braced frames with a vertical link", *Proceedings of the Institution of Civil Engineers - Structures and Buildings*, **170**(11), 1-9. https://doi.org/10.1680/jstbu.16.00100

Ghamari, A., Haeri, H., Khaloo, A. and Zhu, Z. (2019), "Improving the hysteretic behavior of Concentrically Braced Frame (CBF) by a proposed shear damper", *Steel Compos. Struct., Int. J.*, **30**(4), 383-392. https://doi.org/10.12989/scs.2019.30.4.383

Hosseini Hashemi, B. and Moaddab, E. (2017), "Experimental study of a hybrid structural damper for multi-seismic levels", *Proceedings of the Institution of Civil Engineers-Structures and Buildings*, **170**(10), 722-734. https://doi.org/10.1680/jstbu.15.00122

Hossain, M.R. and Ashraf, M. (2012), "Mathematical modelling of yielding shear panel device", *Thin-Wall. Struct.*, **59**, 153-161.

https://doi.org/10.1016/j.tws.2012.04.018
Hossain, M.R., Ashraf, M. and Albermani, F. (2011), "Numerical modelling of yielding shear panel device for passive energy dissipation", *Thin-Wall. Struct.*, **49**(8), 1032-1044. https://doi.org/10.1016/j.tws.2011.03.003
Krawinkler, H. (1992), Guidelines for cyclic seismic testing of components of steel structures (ATC - 24).
Lee, C.H., Ju, Y.K., Min, J.K., Lho, S.H. and Kim, S.D. (2015), "Non-uniform steel strip dampers subjected to cyclic loadings", *Eng. Struct.*, **99**, 192-204. https://doi.org/10.1016/j.engstruct.2015.04.052
Lee, C., Kim, J., Kim, D., Ryu, J. and Ju, Y.K. (2016), "Numerical and experimental analysis of combined behavior of shear- type friction damper and non-uniform strip damper for multi-level seismic protection", *Eng. Struct.*, **114**, 75-92. https://doi.org/10.1016/j.engstruct.2016.02.007
Li, S., Wang, Q.R., Li, X.L. and Tian, J.B. (2020), "Seismic performance of Y-type eccentrically braced frames combined with high-strength steel based on performance-based seismic design", *Struct. Des. Tall Special Build.*, **29**(11). https://doi.org/10.1002/tal.1689
Lian, M. and Su, M. (2017a), "Seismic performance of high-strength steel fabricated eccentrically braced frame with vertical shear link", *J. Constr. Steel Res.*, **137**(10), 262-285. https://doi.org/10.1016/j.jcsr.2017.06.022
Lian, M. and Su, M. (2017b), "Experimental study and simplified analysis of EBF fabricated with high strength steel", *J. Constr. Steel Res.*, **139**(12), 6-17. https://doi.org/10.1016/j.jcsr.2017.09.013
Lian, M. and Su, M. (2017c), "Shake table test of Y-shaped eccentrically braced frames fabricated with high-strength steel", *Earthq. Struct.*, *Int. J.*, **12**(5), 501-503. https://doi.org/10.12989/eas.2017.12.5.501
Lian, M. and Su, M. (2018), "Seismic testing and numerical analysis of Y-shaped eccentrically braced frame made of high-strength steel", *Struct. Des. Tall Special Build.*, **27**(6), e1455. https://doi.org/10.1002/tal.1455
Lian, M., Su, M. and Guo, Y. (2015), "Seismic performance of eccentrically braced frames with high strength steel combination", *Steel Compos. Struct.*, *Int. J.*, **18**(6), 1517-1539. https://doi.org/10.12989/scs.2015.18.6.1517
Lian, M., Su, M. and Guo, Y. (2017), "Experimental performance of Y-shaped eccentrically braced frames fabricated with high strength steel", *Steel Compos. Struct.*, *Int. J.*, **24**(4), 441-453. https://doi.org/10.12989/scs.2017.24.4.441
Mait, D.K., Shyju, P.P. and Vijayaraju, K. (2006), "Vibration control of mechanical systems using semi-active MR-damper", *Smart Struct. Syst.*, *Int. J.*, **2**(1), 61-80. https://doi.org/https://doi.org/10.12989/sss.2006.2.1.061
Makihara, K. (2012), "Energy-efficiency enhancement and displacement-offset elimination for hybrid vibration control", *Smart Struct. Syst.*, *Int. J.*, **10**(3), 193-207. https://doi.org/https://doi.org/10.12989/sss.2012.10.3.193
Nakashima, M., Iwai, S., Iwata, M., Takeuchi, T., Konomi, S., Akazawa, T. and Saburi, K. (1994), "Energy dissipation behaviour of shear panels made of low yield steel", *Earthq. Eng. Struct. Dyn.*, **23**(12), 1299-1313. https://doi.org/10.1002/eqe.4290231203
Oinam, R.M. and Sahoo, D.R. (2018a), "Numerical evaluation of seismic response of soft-story RC frames retrofitted with passive devices", *Bull. Earthq. Eng.*, **16**(2), 983-1006. https://doi.org/10.1007/s10518-017-0240-5
Oinam, R.M. and Sahoo, D.R. (2018b), "Using metallic dampers to improve seismic performance of soft-story RC frames: Experimental and numerical study", *J. Perform. Constr. Facil.*, **33**(1). https://doi.org/10.1061/(ASCE)CF.1943-5509.0001254
Preumont, A. (1999), "Vibration control of active structures: an introduction", *Meccanica*, **34**, 139. https://doi.org/10.1023/A:1004398914135
Rai, D.C., Annam, P.K. and Pradhan, T. (2013), "Seismic testing of steel braced frames with aluminum shear yielding dampers", *Eng. Struct.*, **46**, 737-747. https://doi.org/10.1016/j.engstruct.2012.08.027
Ranaei, O. and Aghakouchak, A.A. (2018), "A new hybrid energy dissipation system with viscoelastic and flexural yielding strips dampers for multi-level vibration control", *Arch. Civil Mech. Eng.*, **19**(2). https://doi.org/10.1016/j.acme.2018.12.005
Roeder, C.R. and Popov, E.P. (1978), "Eccentrically braced steel frames for earthquakes", *J. Struct. Div.*, **104**(3), 391-412. https://doi.org/10.1061/JSDEAG.0004875
Rousta, A.M. and Zahrai, S.M. (2017), "Cyclic testing of innovative two-level control system : Knee brace & vertical link in series in chevron braced steel frames", *Struct. Eng. Mech.*, *Int. J.*, **64**(3), 301-310. https://doi.org/10.12989/sem.2017.64.3.301
Sahoo, D.R., Singhal, T., Taraithia, S.S. and Saini, A. (2015), "Cyclic behavior of shear-and- flexural yielding metallic dampers", *J. Constr. Steel Res.*, **114**, 247-257. https://doi.org/10.1016/j.jcsr.2015.08.006
Seki, M., Katsumata. H., Uchida, H. and Takeda, T. (1988), "Study on earthquake response of two-storied steel frame with Y-shaped braces", *Proceedings of the 9th World Conference on Earthquake Engineering*, Tokyo-Kyoto, Japan.
Silwal, B., Michael, R.J. and Ozbulut, O.E. (2015), "A superelastic viscous damper for enhanced seismic performance of steel moment frames", *Eng. Struct.*, **105**, 152-164. https://doi.org/10.1016/j.engstruct.2015.10.005
Soong, T. and Dargush, G. (1997), *Passive Energy Dissipation Systems in Structural Engineering*, Willey.
Symans, M.D. and Constantinou, M.C. (1999), "Semi-active control systems for seismic protection of structures: a state-of-the-art review", *Eng. Struct.*, **21**(6), 469-487. https://doi.org/10.1016/S0141-0296(97)00225-3
Wei, B., Li, C., Jia, X., He, X. and Yang, M. (2019), "Effects of shear keys on seismic performance of an isolation system", *Smart Struct. Syst.*, *Int. J.*, **24**(3), 345-360. https://doi.org/10.12989/sss.2019.24.3.345
Ying, Z.G., Ni, Y.Q. and Ko, J.M. (2009), "A semi-active stochastic optimal control strategy for nonlinear structural systems with MR dampers", *Smart Struct. Syst.*, *Int. J.*, **5**(1), 69-79. https://doi.org/10.12989/sss.2009.5.1.069
Zahrai, S.M. (2015), "Cyclic testing of chevron braced steel frames with IPE shear panels", *Steel Compos. Struct.*, *Int. J.*, **19**(5), 1167-1184. https://doi.org/10.12989/scs.2015.19.5.1167
Zahrai, S.M. and Bruneau, M. (1999), "Ductile end-diaphragm for seismic retrofit of slab-on-girder steel bridges", *J. Struct. Eng.*, **125**(1), 71-80. https://doi.org/10.1061/(ASCE)0733-9445(1999)125:1(71)
Zahrai, S.M. and Cheraghi, A. (2017a), "Improving cyclic behavior of multi - level pipe damper using infill or slit diaphragm inside inner pipe", *Struct. Eng. Mech.*, *Int. J.*, **64**(2), 195-204. https://doi.org/10.12989/sem.2017.64.2.195
Zahrai, S.M. and Cheraghi, A. (2017b), "Reducing seismic vibrations of typical steel buildings using new multi-level yielding pipe damper", *Int. J. Steel Struct.*, **17**(3), 1-16. https://doi.org/10.1007/s13296-017-9010-0
Zahrai, S.M. and Jalali, M. (2014), "Experimental and analytical investigations on seismic behavior of ductile steel knee braced frames", *Steel Compos. Struct.*, *Int. J.*, **16**(1), 1-21. https://doi.org/10.12989/scs.2014.16.1.001
Zahrai, S.M. and Moslehi Tabar, A. (2006), "Cyclic Behavior of Steel Braced Frames Using Shear Panel System", *Asian J. Civil Eng.*, **7**(1), 13-26.
Zahrai, S.M. and Moslehi Tabar, A. (2013), "Analytical study on

cyclic behavior of chevron braced frames with shear panel system considering post-yield deformation", *Can. J. Civil Eng.*, **40**(7), 633-643. https://doi.org/10.1139/cjce-2012-0430

Zahrai, S.M. and Vosooq, A.K. (2013), "Study of an innovative two-stage control system : Chevron knee bracing & shear panel in series connection", *Struct. Eng. Mech., Int. J.*, **47**(6), 881-898. https://doi.org/10.12989/sem.2013.47.6.881

HJ